Transactions of the 15th International Conference on
Structural Mechanics in Reactor Technology (SMiRT-15)
Seoul, Korea, August 15-20, 1999

Dynamic Responses of Plates and Cylinders Impacted with Detonation Gases Initiated Using Wire Explosion Techniques

Tetsuyuki Hiroe, Kazuhito Fujiwara, Hideo Matsuo, Yasunobu Araki and Daisuke Nakayama

Kumamoto University, Japan

ABSTRACT Dynamic responses of metallic plates and cylinders impacted with planar and cylindrically diverging detonation gases of powder PETN have been investigated respectively, using diagnostic tools and hydro codes for shock propagation and high-strain-rate phenomena. The plane detonation waves initiated by exploding wire-rows generate triangular-shaped pressure pulses in plates, inducing spall or scab fracture, and the cylindrical detonation waves initiated by a wire-explosion at the central axis expand cylinders uniformly and rapidly with the strain rate of above 10^4 s^{-1}. Comparisons of experimental observations and numerical simulations indicate that the developed explosive devices are applicable to study not only detonation-structure interactions but also dynamic behavior of materials.

INTRODUCTION

The understanding of high-strain-rate deformation and fracture of materials and structures is very important in the studies on high-speed fabrication, accidental impact of vehicles and crashworthiness shielding, blast of containers for high-energy storage and earthquake responses. Explosive loading devices had been developed as simple experimental methods to supply impulsive loads for the study of dynamic processes. In order to generate planar or cylindrical detonation waves used as basic loadings, various explosive assembly systems[1] have been required to transform a point detonation initiated by a detonator. A unique wave generator was developed[2] and it has been extended for implosion of solids[2, 3]. In this wave generator, cylindrical shell of powder pentaerithritoltetranitrate (PETN) is initiated by the simultaneous explosion of parallel copper wire rows or etched copper mesh placed over the entire outer surface using an impulsive discharge current from a capacitor bank. Such initiation technique of PETN powder seems to be adopted rather simply to some other types of shock loadings. The present paper introduces the generation of planar and cylindrically diverging waves and the applications to dynamic responses of plates and cylinders using this wire-explosion technique.

Among the various plane wave generators, the explosive lens systems are the most common, where the surface planar initiation of the main charge is achieved after the detonation of conical explosive assembly. The proposed generator produces planar detonation front in the PETN layer immediately after the initial explosion of wire-rows and transfers an one-dimensional triangular pressure pulse to the specimen. In preliminary study[2], the configuration of wire-rows and the PETN for the generation of planar detonation wave are investigated and the generator is adopted to perform the spall tests for plate specimens of

metals. Previously[4], the spall damages had been observed after the tests by cutting the recovered specimens involving secondary damages and deformation. In this study, the damages are recorded in-situ by measuring free surface velocity traces with use of a laser interferometry system. The experimental results are compared with numerical results. The other type of explosive loading is developed for a rapid expansion of cylinders. Usually, axially phased cylinder expansion tests had been conducted. In the proposed device, a PETN column is initiated at the central axis simultaneously by exploding a wire, producing cylindrically diverging detonation wave[5]. Then the detonation gas expands a cylinder specimen installed coaxially outside the PETN column uniformly. The deformation phenomenon is observed using a high-speed camera and the laser interferometry system. The experimental results are examined with numerical simulations using typical stress-strain models for high-strain-rate phenomena.

DEVELOPMENT OF EXPLOSIVE LOADING DEVICES

The experiments were performed utilizing the facilities at the High Energy Rate Laboratory, Kumamoto University. Figure 1 shows the schematic applications of wire-explosion techniques used so far for three kinds of explosive loadings. In all the loadings, dry powder PETN with the charge density of around 0.95 g/cc is initiated by exploding the fine copper wires with the diameter of 175 μm using a capacitor bank of 40 μF, 20 kV. The discharge current is monitored with the Rogowskii coil.

The plane wave generator consists of the PETN and its box-container which has parallel copper wire rows placed on the inner bottom surface and the electrodes for the current supply from the capacitor bank. Planar detonation is achieved as shown in Fig. 1A after the interference process of embryo detonation between neighboring wires. As a preliminary study, the relations of peak current per wire, wire-row numbers, intervals B, PETN thicknesses H and arrival time jitters of detonation waves were investigated[2] measuring arrival time jitters of detonation waves. The wire conditions H/B>1.3～1.5 fitting to required planarity of detonation front (time-jitter: ±0.1 μs) were obtained from the detonation tests for the PETN of 25～70 cm^2 area. When a plate specimen is set in contact with the surface of the PETN, one-dimensional triangular-shaped pressure pulse is transferred to the plate. The shock wave is reflected at the free surface and soon spalling occurs due to internal tensile stresses generated by the interaction of rarefaction waves. The inclination and height of the stress distribution are related with the thickness of the PETN and the shock impedance of the specimen. Schematics of developed explosive assembly for spall test is shown in Fig. 2.

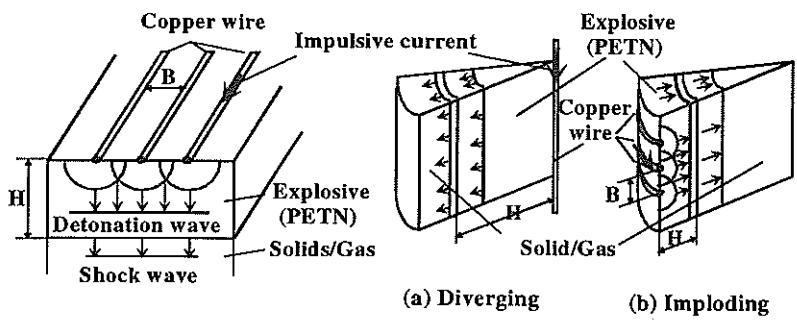

Fig. 1 Generation of fundamental detonation waves using wire-explosion techniques

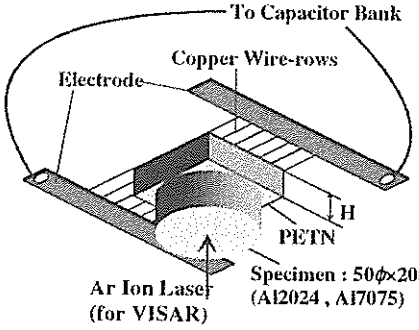

Fig. 2 Application of plane detonation waves to spall tests for metal plates

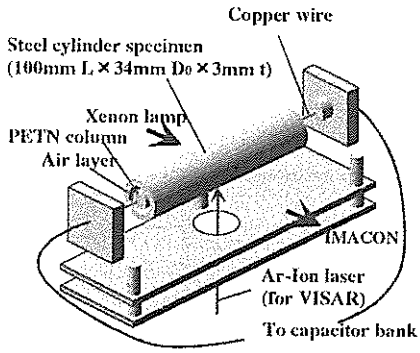

Fig. 3 Application of cylindrical diverging detonation waves to rapid expansion

The cylindrical diverging wave generator consists of a column of the PETN and a copper wire set at the central axis of the column. Exploding the wire simultaneously produces axially uniform expanding detonation. Prior to the cylinder expansion tests, three types of explosive charged test assembly[5] are provided to investigate the conditions of the wire and the PETN configuration. Axial and circumferential arrival-time-jitters were recorded for the PETN columns with various lengths and diameters using a streak camera. In other test, radius run distance for stable diverging detonation is observed recording the light from a meridian line of a conical PETN container. As the results, it was known that the cylindrical diverging detonation waves generated in this study have circumferential and axial uniformity within the time-jitter of ±0.3-0.4 μs when the length of the PETN column is less than 240-290 mm and the diameter is more than 8-10 mm. The critical discharge current value under suitable condition is around 40 kA. Schematics of test setup for the uniform expansion of cylinders is shown in Fig. 3, where the air-layer is placed as an attenuator.

SPALL FRACTURE OF PLATES IMPACTED WITH DETONATION GASES

The developed plane wave generator is adopted to spall the plate specimens of Al 2024 and Al 7075 with the size of 50^{ϕ}x20^{t} mm. The PETN is charged to the thicknesses H of 10, 15, 20 mm. Some specimens are recovered with rather little damage using a water pool or buffer. However, all the recovered specimens had considerable secondary damages such as deformation and crack closure. Then, as an in-situ measurement, a laser interferometry system (ATA fixed cavity VISAR model 605) has been adopted to observe the free surface-velocity histories of the specimens. Figure 4 shows the schematic diagram of the laser interferometer system combined with the spalling test assembly. An Ar-ion laser generator (1.5W: single line) is placed apart from the explosive setup in the pit and they are connected using mirrors, lens and fibers. Etalons with the fringe constants of 309.6 (delay unit I) and 108.1 (delay unit II) m/s/fringe are provided for the tests. In the spalling tests, the free surface velocity jumps abruptly and the lost fringe has to be placed in front of the plastic wave in the data analysis. The initial loading profile resulting from the detonation of the explosive is triangular-like in shape, with the rate of pressure decay from the shock front being a function of PETN height or thickness. The pressure pulse transferred to the specimen is reflected back as a release wave at the free surface. It interacts with another release waves coming from the inner surface of the explosive and generates internal tensile stresses, producing spalling failure in the plate specimen. The spall model induced by explosive-plate interaction is

illustrated with a predicted VISAR signal in Fig. 5. One-dimensional plane wave region for spall evaluation is estimated[4] within 7 mm in depth from the free surface at the central axis.

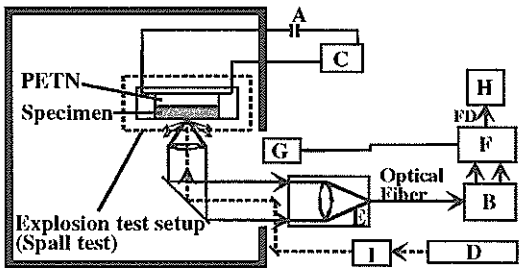

A: Capacitor bank
B: Fixed-cavity VISAR (ATA Model 605)
C: Control box
D: Ar-Ion laser
E: Laser collection system
F: Digital memory
G: Photo cell
H: Data analysis routine
I: Spectrum Analyzer

Fig. 4 Experimental block diagram for spall tests for plates and VISAR system

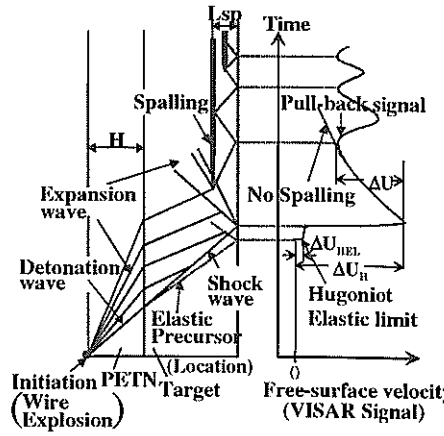

Fig. 5 Spall model in plate induced by explosive shock loading

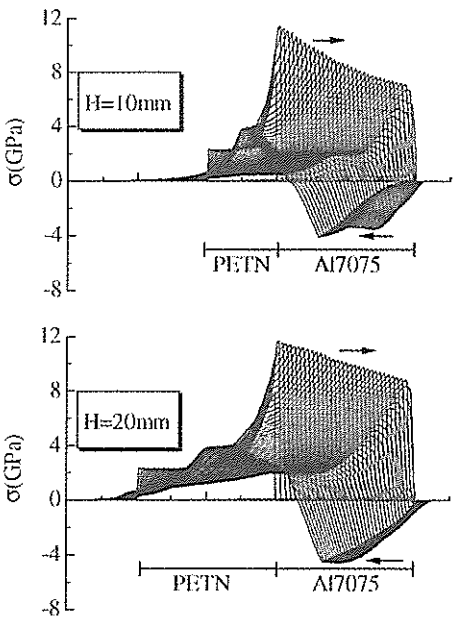

Fig. 6 Numerical spatial distributions of normal stress in Al7075 plates at intervals of 0.1μs

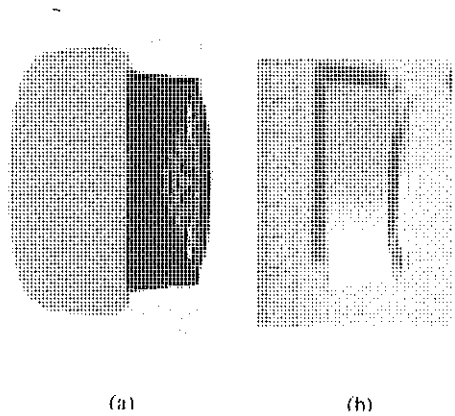

Fig. 7 Comparison of spall damage in cross-sections of plates between: (a) a numerical result by AUTODYN-2D for Al7075 (PETN thickness: 10mm) and (b) an experimental result obtained from a recovered specimen.

Spatial distributions of normal stresses in Al 7075 for H: 10, 20mm are calculated using the 1-D Lagrangian FDM code based on Wondy IIIa[6] as shown in Fig. 6. Numerical analysis shows the obvious effect of PETN height H on the peak stress attenuation during the transmission of shock waves across the specimens. In addition, a two-dimensional hydro code: AUTODYN-2D ver. 28 is also adopted to simulate damages of the entire specimen, using Euler formulation and stress criterion for spall. Mie-Grüneisen EOS and Steinberg[7] constitutive model were employed for aluminum alloy materials in both 1-D and 2-D analysis, where immediate stable plane detonation is assumed with burn model for PETN after wire explosion, using the EOS of perfect gas (1-D) and JWL (2-D). Figure 7 depicts the comparison of spall damages in cross-sections of Al 7075 plates between a 2-D numerical result (spall stress: 2.2GPa) and an experimental result obtained from a recovered specimen for H: 10mm. Both macroscopic damages coincide basically.

Figure 8 and 9 shows the free-surface velocity signals observed by the VISAR and simulated by 1-D analysis for Al 2024 and Al 7075 respectively. The surface velocity rises abruptly after the initial elastic precursor and drops immediately without duration, and the amplitudes of surface-velocity becomes larger for thicker PETN, as predicted in Fig. 6. It is seen that the observed signals for Al 2024 are classified into two types of (a): type II for H: 10, 20mm and (b): type I for H: 15mm as shown in Fig. 8. On the other hand, those for Al 7075 in Fig. 9 belong to only type I. The type II signals reveal the occurrence of incomplete spall or crack nucleation near the free surface prior to the following explicit spall failure. And the type I signals indicate the occurrence of explicit spall near the surface after an embryo time. It seems statistical which type of spall occurs for Al 2024.

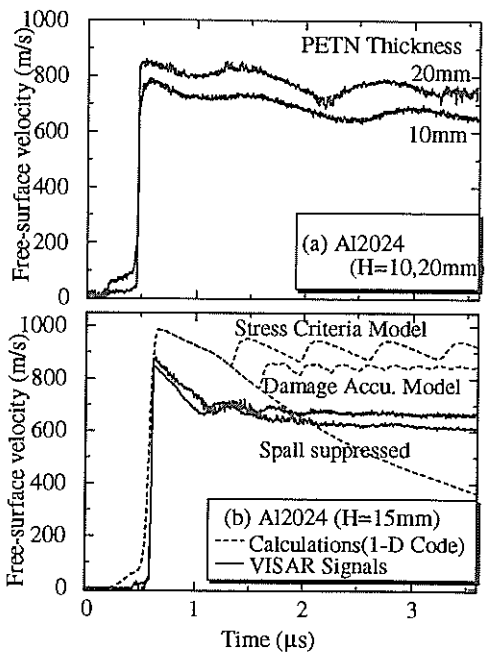

Fig. 8 Free-surface-velocity - time histories for Al2024 plates. (a) VISAR signals (PETN thickness H: 10, 20mm) (b) VISAR signals and numerical simulations (H: 15mm).

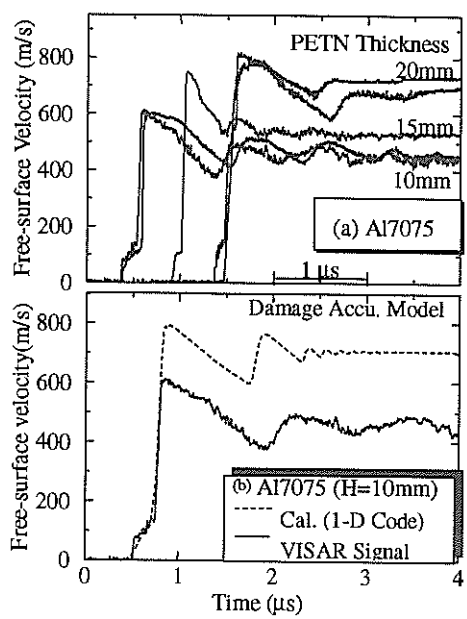

Fig. 9 Free-surface velocity - time histories for Al7075 plates. (a) VISAR signals (PETN thickness H: 10, 15, 20mm) (b) a VISAR signal and a numerical simulation (H:15mm)

The standard spall parameters for Al 2024: spall strength σ_{SP} (II: 1.20, 1.35GPa, I: 1.72GPa), Hugoniot elastic limit σ_{HEL} (0.4-0.5GPa), spall-layer thickness Lsp (II: 2.8, 3.5mm, I: 1.3mm) damage ratio D (II: 0.9, 1.0, I: 0.8)were obtained, using the equations $\sigma_{SP}=0.5\rho_0 C_B \delta U$, $\sigma_{HEL}=0.5\rho_0 C_B \delta U_{HEL}$, $L_{SP}=0.5 C_B \delta t$, D: ratio of pull-backed velocity to peak velocity, where ρ_0: reference density, C_B: bulk sound velocity, δU: pullback velocity, δU_{HEL}: HEL velocity, δt: pullback wave length. The corresponding values for Al 7075 are σ_{SP}: 1.3-1.6GPa, σ_{HEL}: 0.7-1.0GPa, L_{SP}: 0.94-2.38mm, D: 0.80-0.85. In Fig.8 (b) of Al 2024, H: 15mm, almost same experimental results using delay units with different sensitivities are compared with 1-D numerical results for three cases based on stress criteria, damage accumulation model[8] (DAM) and no spalling. In Fig. 9(b) of Al 7075, H: 10mm, the DAM is used for numerical simulation. The DAM is a time-dependent model and expressed as follows:

$$K_{cr} = \int_0^t (\sigma - \sigma_0)^{\lambda} dt, \qquad t: \text{elapsed time of normal tensile stress } \sigma < \sigma_0 < 0$$

,where K_{cr}: 2×10^{-5}, λ : 0.8, σ_0: 0 for Al 2024 and K_{cr}: 5×10^{-6}, λ : 0.4, σ_0: 0 for Al 7075 in kgf-mm-s units. The calculation produces larger velocity values than those of experiments, because the instantaneous complete detonation is assumed at the wire-row plane, ignoring the interaction zone or run-distance in the initial detonation. In the present calculations, the simple DAM reproduces the basic feature of ohserved type I signals, and it suggests a possibility of getting a good agreement with both types of failure modes, incorporating further sophisticated damage models and taking initial interaction of PETN detonation into simulation. So far, the 2-D code in the Euler formulation has not simulated the experimental velocity-histories well.

EXPANSION OF CYLINDERS DRIVEN BY DIVERGING DETONATION GASES

Test specimens were provided from a mild steel tube of 0.14% carbon contents (JIS SGP-E-G) and an 18Cr-8Ni stainless steel tube (JIS SUS 304) with the length of 100 mm, outer

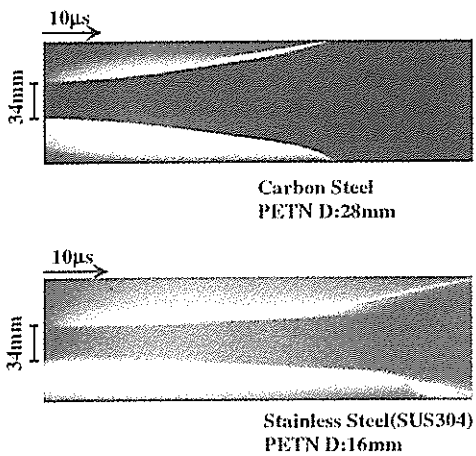

Fig. 10 Typical streak records of expanding cylinder specimens: (a) carbon steel, PETN diameter D: 28mm, (b) stainless steel SUS304, PETN D: 16mm.

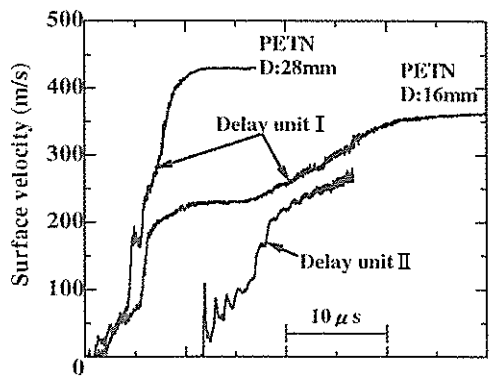

Fig. 11 Time histories of surface velocity for carbon steel cylinders: VISAR signals

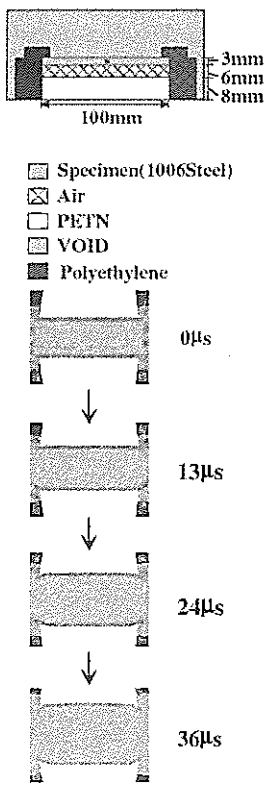

Fig. 12 Typical numerical result of cylinder expansion behavior by AUTODYN-2D (carbon steel, PETN D: 16mm).

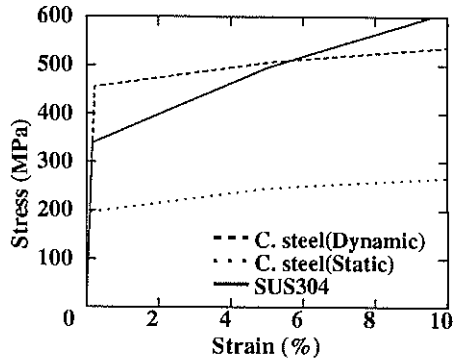

Fig. 13 Stress-strain relations of carbon steel and SUS304 used for 1-D numerical simulations of expanding cylinders

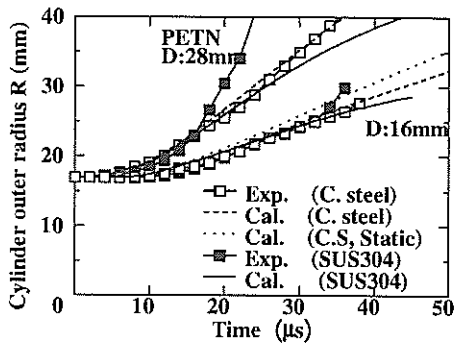

Fig. 14 Experimental and 1-D numerical time-histories of expanding cylinder wall radii at mid-length of the cylinders

diameter of 34 mm and wall thickness of 3 mm. The specimens are installed coaxially outside the PETN columns with diameters D of 16, 28 mm as shown in Fig. 3. In case of D: 16 mm, there is an air-layer of 6 mm between the explosive and the cylinder specimen. Expanding shadows of the specimens are recorded with the high-speed camera system of IMACON 790 and a CCD camera, using a Xenon lamp as a light source behind the specimen. The VISAR system is also adopted to monitor the precise behavior of surface velocity. Typical streak records of expanding diameters up to the final burst stage at the mid-length of cylinders are shown for a carbon steel specimen with PETN of D: 28 mm and a SUS 304 specimen with PETN of D: 16 mm in Fig. 10 (a) and (b) respectively. The records represent that the radial displacements increase symmetrically at nearly a constant velocity after the initial acceleration. The average wall velocity and circumferential logarithmic strain rate are calculated from the mean value of $\dot{R}$ and $\dot{R}/R$ during the expansion at the nearly constant wall velocity, where R is the outer radius of the specimen and dots denote differentiation with respect to time. The average values are almost same for carbon steel and 304 steel, and 340, 700 m/s (velocity: $\dot{R}$) and 1.6, 2.4 x10^4 s^{-1} (strain rate: $\dot{R}/R$) for PETN D: 16 and 28 mm,

respectively. The observed wall velocities are less than 40 % of those by the Gurney equation[9]. The discrepancy comes from the fact that the equation ignores wave propagation effects and the energy consumption in deformation and fracture. The final burst starts rather early for 304 steels. The burst strains $\ln(R_f/R_o)$ of 30-40 % are estimated from the streak records for 304 specimens. The framing photos also have shown axially uniform expansion of cylinders without any axial deformation. Figure 11 shows observed VISAR signals during the acceleration terms for carbon steel specimens. The vibration signal especially with use of sensitive delay unit II indicate the initial cyclic reflections of stress waves in the cylinder wall and wave length corresponds with wall thickness.

The numerical simulations are performed using 2-D and 1-D codes. In the former and latter calculations, Johnson-Cook's constitutive model[10] of 1006 steel and stepwise linear work-hardening model with the strain rate effect of 0.14% carbon steel[11] are applied for carbon steel specimens, and the Steinberg model is adopted for 304 specimens. Figure 12 shows typical 2-D numerical result for the carbon steel specimen with PETN D: 16 mm, expressing that the axial deformation is negligibly small during the cylinder expansion. The dynamic stress-strain curves used in 1-D calculations are compared in Fig. 13. It is predicted that the flow stress of 304 specimen increase swiftly due to the strain hardening enough to cause the cylinder burst early according to the Taylor theory[12]. Figure 14 represents experimental and numerical time-histories of expanding wall radii. The numerical diagrams show a fairy good agreement with the experimental curves and the strain-rate effect of material on cylinder expansion behavior.

As the results, proposed explosive loading techniques are available to obtain the fundamental data on dynamic fracture of plates and rapid expansion of cylinders.

1. Meyers, M. A., *Dynamic Behavior of Materials*, John Wiley & Sons Inc., 1994.
2. Hiroe, T., Matsuo, H., Fujiwara, K., Yoshida, M., Fujiwara, S., Miyata, M., Sakai, S., Fukano, T. and Abe, T., "A study on generation of plane detonation and strong imploding shocks by wire-row explosion", *J. of the Japan Explosive Society*, Vol. 57, No. 2, 1996, pp.49-54.
3. Abe, T., Yoshida, M., Hiroe, T., Fujiwara, K. and Matsuo, H., "Explosive-Driven Cylindrical Imploding Shocks in Solid Initiated with an Exploded Etched Copper Mesh", *Proc. of Int. Conf. AIRAPT-16 and HPCJ-38 on High Pressure Science and Tech.*, Vol. 7, pp. 912-914, Kyoto, Japan, August, 1997.
4. Hiroe, T., Matsuo, H., Fujiwara, K., Miyata, M., Matsumoto, S., Abe, T., "Spall in Metals Induced by Explosive Shock Loadings and Protective Measures Using Momentum Traps", *Trans. Japan Society of Mechanical Engineers, Ser. A*, Vol. 62, 1996, pp. 2026-2031.
5. Hiroe, T., Matsuo, H., Fujiwara, Abe, T. and Kusumegi, K., "Uniform Expansion of Cylinders at High Strain Rates using an Explosive Loading", *Proc. of Int. Conf. on Condensed Matter under High Pressures*, pp. 458-465, Bombay, India, Nov., 1996.
6. Lawrence, R. J., "Wondy IIIa, A Computer Program for One-dimensional Wave Propagation", *Sandia Laboratory Development Report*, No. 70-315, 1970.
7. Steinberg, D. J., Cochran, S. G. and Guinan, M. W., "A Constitutive Model for Metals Applicable at High-Strain Rate", *J. Appl. Phys.*, Vol. 51, 1980, pp. 1498-1504.
8. Tuler, F. and Butcher, B. M., "Criterion for the Time Dependence of Dynamic Fracture", *Int. J. Fract. Mech.*, Vol. 4, 1968, pp. 431-437.
9. Gurney, R., "The Initial Velocities of Fragments from Bombs, Shells and Grenades", *Ballistic Research Laboratory Report* No. 405, September 1943.
10. Johnson, G. R. and Cook, W. H., "A Constitutive Model and Data for Metals Subjected to Large Strains, High Strain Rates, Temperatures and Pressures", *Proc. 7th Int. Symp. on Ballistics*, pp. 541-547, The Hague, The Netherlands, 1983.
11. JSME, "Investigation Report on Impact and Fracture", *JSME Subcommittee Report* No. 294, 1981.
12. Grady, D. E. and Hightower, M. M., "Natural Fragmentation of Exploding Cylinders", *Shock-wave and high-strain-rate phenomena in materials*, edited by M. A. Meyers, et al., Marcel Dekker, Inc., 1992, pp.713-721.